Full paper

Applied
Organometallic
Chemistry

Received: 15 June 2015 Revised: 31 July 2015 Accepted: 19 August 2015 Published online in Wiley Online Library: 26 October 2015

(wileyonlinelibrary.com) DOI 10.1002/aoc.3389

New palladium catalyst immobilized on epoxy resin: synthesis, characterization and catalytic activity

Natalia Sienkiewicz[a]*, Krzysztof Strzelec[a], Piotr Pospiech[b], Marek Cypryk[b] and Tomasz Szmechtyk[a]

A new thiol-functionalized epoxy resin as a support for palladium(II) complexes has been synthesized in good yields. A palladium catalyst was 'heterogenized' by anchoring [$PdCl_2(PhCN)_2$] complexes to these thiol-functionalized polymers via ligand exchange reaction. These new palladium catalysts were tested in Mizoroki–Heck coupling and hydrogenation reactions. The activity of the complexes in terms of yield is comparable to that of homogeneous $PdCl_2(PhCN)_2$. The stability and a good recycling efficiency of these catalysts make them useful for prolonged use. The constant and good selectivity of the supported catalysts during recycling experiments indicate that they could be useful for practical application in many organic reactions. To characterize the heterogeneous complexes before and after use, X-ray photoelectron spectroscopy, infrared spectroscopy, scanning electron microscopy, energy dispersive X-ray microscopy, atomic absorption spectroscopy and time-of-flight secondary ion mass spectrometry were applied. Density functional theory calculations were also used to better understand the structures of the obtained palladium complexes. Polythiourethanes contain three atoms, oxygen, nitrogen and sulfur, capable of coordinating to transition metals. We examined the possibility of intra- and intermolecular binding for both *cis* and *trans* palladium complexes. Copyright © 2015 John Wiley & Sons, Ltd.

Additional supporting information may be found in the online version of this article at the publisher's web-site.

Keywords: heterogeneous catalysts; properties and characterization; epoxy resins; polythiourethanes; structure–property relations; hydrogenation reaction; Mizoroki–Heck reaction

Introduction

Epoxy resins have a set of unique properties that are not commonly found in other plastic materials, such as excellent mechanical strength, outstanding chemical, moisture and corrosion resistance, good thermal, adhesive and electrical properties, dimensional stability (i.e. low shrinkage upon curing) and a lack of volatile emissions.[1–3] Epoxy resins, because of these characteristics, are also used as carriers for catalysts in many important organic reactions, in the industrial production of several commodity compounds, as well as in the synthesis of many intermediates, fine chemicals and pharmaceuticals. For example, catalysts with unprecedented long-term activities in the range of at least some months have been obtained by the use of thermosetting epoxy resins as supports. These catalysts are prepared in a convenient one-step procedure employing metal complexes that act simultaneously as polymerization indicators as well as precursors for catalytically active species in the resulting polymers. With respect to polymeric supports, it should be pointed out that about 65% of the reviewed heterogenized catalyst systems are based on polystyrene, polymethacrylate and poly(ethylene glycol). Furthermore, hybrid catalyst systems comprising organic polymers together with inorganic components, such as recently reported titanium catalysts based on polystyrene–silica or molybdenum catalysts supported on epoxy resin–silica composites, offer new possibilities for the development of efficient polymer-supported catalysts.[4] Thiol-functionalized epoxies have proved to be very convenient for stabilizing enzymes by multipoint immobilization. Their use allows not only the specific immobilization of enzymes through their thiol groups by thiol–disulfide interchange, but also enzyme stabilization through covalent attachment.[5] Epoxy resins with amine and mercaptan chelating groups have been prepared by the suspended condensation polymerization of 2-chloroethoxymethyl thiirane and diamines. The resins show high affinity for noble metal ions and Hg(II), and predominantly adsorb Pd(II) or Hg(II) in the presence of Cu(II), Zn(II) and Mg(II) ions.[6] Dodecylthiolate-stabilized palladium nanoparticles have been shown to be active catalysts for the formation of carbon nanotubes.[7] Furthermore, they have been demonstrated to be stable and recyclable catalysts in the Suzuki–Miyaura C–C coupling reaction of halogenoarenes and phenylboronic acid,[8] while thiolated β-cyclodextrin-stabilized palladium nanoparticles have shown good activity in the hydrogenation of allylamine.[9] Palladium nanoparticles stabilized by BINAP–thioether derivatives have also been used in (quasi) homogeneous C–C coupling reactions.[10] The presence of a chelating diphosphine ligand provides

---

* Correspondence to: Natalia Sienkiewicz, Institute of Polymer and Dye Technology, Faculty of Chemistry, Lodz University of Technology, Stefanowskiego 12/16, 90-924 Lodz, Poland. E-mail: natalia.sienkiewicz@p.lodz.pl

a Institute of Polymer and Dye Technology, Faculty of Chemistry, Lodz University of Technology, Stefanowskiego 12/16, 90-924, Lodz, Poland

b Center of Molecular and Macromolecular Studies, Polish Academy of Sciences, Sienkiewicza 112, 90-363, Lodz, Poland

remarkable stability to the nanoparticles, preventing their aggregation throughout the process. Furthermore, the nanoparticles could be subsequently isolated and reused without any loss of catalytic activity.

In our earlier works, we used thiirane resins cured with polythiourethane (PTU) hardeners which are very useful and versatile polymeric supports for the preparation of heterogenized palladium catalysts for the Heck reaction.[11] The use of PTUs as curing agents enables one to obtain supports that do not need any further functionalization. The different coordination sites in the polymer promote the formation of active catalytic species mainly as finely dispersed metal particles with mixed valence states. The chemical structure of the PTU oligomers used can greatly affect the activity of the catalysts. Polymers or metal–organic frameworks as some of the essences of crystal engineering and coordination chemistry have attracted considerable attention from chemists, physicists and materials scientists for the development of hybrid crystalline solids with novel supramolecular structures and physicochemical properties. Supported-metal catalysts are among the most important materials in heterogeneous catalysis.

In this report, we present a method for the coordination of a palladium catalyst on a support prepared from an epoxy resin cured with thiol-terminated PTU. In recent decades there has been considerable progress in the application of quantum chemical calculations to define the structures of catalysts, as well as to solve problems in homogeneous and heterogeneous catalysis.[12–15] The rapid increase in computing power and the development of computational algorithms allow one to perform calculations of the structures and properties of transition metal complexes. It is known that computational methods can help to explain the mechanisms of catalysis involving transition metals. In the work reported here, density functional theory (DFT) methods were applied to better understand the geometries of the investigated catalytic systems. The oligomeric PTUs, apart from their good curing characteristic of epoxides, allow the introduction of new binding ligands into the structure of the polymer. The activity of these new catalysts was investigated in Mizoroki–Heck and hydrogenation reactions.

Experimental

Materials

All organic solvents used in this study were supplied by Sigma-Aldrich and were used without further purification. The commercially available epoxy resin (diglycidyl ether of bisphenol A) Epidian-5 (EP5), having epoxide number of 0.487, was obtained from Organika-Sarzyna, Poland. The viscosity of the resin was 23.9 N s m^{-2} at 25°C. PTU hardeners were prepared by the reaction of hexamethylene diisocyanate and pentaerythritol tetrakis(3-mercaptopropionate) and 3,6-dioxa-1,8-octanedithiol which were purchased from Sigma-Aldrich and used without further treatment. $PdCl_2(PhCN)_2$ was prepared from $PdCl_2$ (Sigma-Aldrich, 98%) and benzonitrile (Sigma-Aldrich, 99%).[16]

Preparation of new thiol-functionalized epoxy resin

The carrier was prepared by mixing the epoxy resin (3 g) with either difunctional PTU (DPTU; Fig. 1) or multifunctional PTU (MPTU; Fig. 2) hardener (40 wt%). The Fourier transform infrared (FT-IR), ^{1}H NMR and gel permeation chromatography analyses of the cross-linked resins were performed in our previous work.[17] After obtaining homogenous consistency, the mixture was transferred onto a Teflon® mould and cured at a room temperature over a period of 1–2 h. For all cured samples, 0.01% of 2,4,6-tris(dimethylaminomethyl)phenol (DMP-30) was used as an accelerator. The cured resin was frozen by immersion in liquid nitrogen and mechanically ground to powder. The particle size was about 0.5 mm which was determined using sieve analysis.

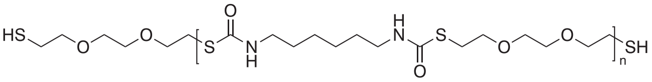

Figure 1. Difunctional polythiourethane (DPTU).

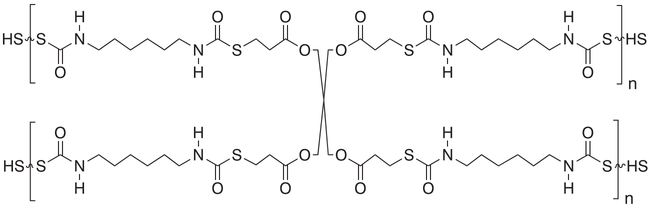

Figure 2. Multifunctional polythiourethane (MPTU).

Preparation of heterogenized palladium complexes

A typical procedure was as follows. On the prepared resin matrix, we immobilized the palladium complex $PdCl_2(PhCN)_2$ from toluene solution, using a ligand-exchange process. To a known amount of suitable resin (0.5 g) in a round-bottom flask, $PdCl_2(PdCN)_2$ dissolved in 10 ml of toluene was added. The palladium content for all supported catalysts was fixed below the metal maximum uptake capacity for a polymer, which was also confirmed from atomic absorption spectroscopy (AAS) analysis of the colourless toluene solutions after the immobilization process. The mixture was stirred at room temperature for 3 days, with a change of the compound colour from dark brown to slightly yellowish indicating that the palladium complex had reacted with the prepared polymer. The yellow product was filtered off, extracted with toluene under nitrogen in order to remove any complex that was non-chemically bound to the polymer matrix, and finally dried under vacuum.

Structural characterization

FT-IR spectra were recorded with a BIORAD FT-IR 175C spectrophotometer in an air atmosphere. A polymer sample was mixed with KBr using the snap-reflection technique for DRIFT measuring. Bonding nature of the catalyst surface was investigated using X-ray photoelectron spectroscopy (XPS). XPS measurements were made using a VG ESCALAB 210 spectrometer with Mg Kα (1253.6 eV) excitation from an X-ray tube (reduced power, 10 kV, 10 mA). The pressure in the spectrometer chamber was about 10^{-9} mbar. Samples were pressed to pellets under a pressure of 100 kbar for 10 min before measurements. The C 1s, N 1s, O 1s, Cl 2p, S 2p and Pd 3d core level spectra were recorded. The analyser pass energy was set at 20 eV. A take-off angle of 90° was used in all XPS studies. Curve fitting was performed using the ECLIPSE data system software. This software describes each of the components of a complex envelope as a Gaussian–Lorentzian sum function. The background was fitted using nonlinear model function proportional to the

Copyright © 2015 John Wiley & Sons, Ltd.

integral of the elastically scattered electrons. All binding energies were referenced to the C 1s neutral carbon peak at 284.6 eV.

The Heck and hydrogenation reaction products were quantitatively analysed using GC with a Hewlett-Packard 5990 II gas chromatograph equipped with a thermal conductivity detector. The GC column was an HP-50+ (cross-linked 50% PhMe silicone; 30 m × 0.63 mm × 1.0 μm film thickness). Reagents were identified based on previously determined retention times. The Heck reaction yield was determined from the loss of iodobenzene relative to a standard (toluene) at a time. The retention times of reagents for the above conditions of operation of the column were determined experimentally: iodobenzene, 9.991 min; methyl acrylate, triethylamine, *N*-methylpyrrolidone, 12.693 min; toluene, 2.141 min; *trans*-methyl cinnamate, 20.132 min. GC operating conditions: injector and detector temperature, 210°C; carrier gas, helium. Temperature programme: the column was maintained at 50°C for 2 min, then heated to 150°C at a rate of 5°C min^{-1}. For the hydrogenation reaction, the GC operating conditions were: injector and detector temperature, 210°C; carrier gas, helium. Temperature programme: the column was maintained at 50°C for 3 min, then heated to 140°C at a rate of 70°C min^{-1}. The retention times of reagents for the above conditions of operation of the column were determined experimentally: *trans*-cinnamic aldehyde, 6.948 min; toluene, 2.117 min; ethanol, 0.657 min.

The amount of palladium loaded in the support was analysed using AAS with a PerkinElmer 3030 atomic absorption spectrometer. A sample of a polymer-supported catalyst was heated to 600°C and then dissolved in aqua regia. The resulting solution was diluted and assayed using AAS.

Time-of-flight secondary ion mass spectrometry (ToF-SIMS) measurements were made using an ION-TOF GmbH instrument (ToF-SIMS IV) equipped with a 25 keV pulsed Bi1 primary ion gun in the static mode (primary ion dose about 1.5×10^{11} ions cm^{-2}). The analysed area corresponded to a square of 500 μm × 500 μm in the case of secondary ion mass spectra collecting and surface imaging. For each prepared sample, three spectra from different surfaces areas were obtained. To obtain a plain surface of catalysts (then better mass resolution could be achieved), powder samples were tableted before the measurements. In order to compare the quantity of palladium present on the surface of 'fresh' and 'used' catalysts, the number of counts of selected ions obtained from collected mass spectra was normalized on the basis of the value of total counts.

The morphology of samples was investigated with a scanning electron microscopy (SEM) instrument (JEOL 5500 LV), working at high vacuum and an accelerating voltage of 10 kV. Energy dispersive X-ray spectroscopy (EDX) SEM microscope (JEOL JSM 840A, Japan) was used to observe the elemental distribution. The white points in the figures denote Pd atoms. Pore size distribution parameters were determined by application of the BET method using a Sorptomatic 1900 instrument (Fisons).

Computational studies

The calculations were performed using the Gaussian 03 and Spartan '08 programs.[18,19] The starting structures for geometry optimization were obtained from conformational search using the MMFF method with Spartan. Geometry optimizations (Gaussian 03) in the gas phase were carried out using the M06-2X density functional[20] and the 6-31G* basis set for H, C, O, Cl, N and S and the effective core potential basis set LANL2DZ for Pd. All equilibrium structures were identified by frequency calculations. Thermal corrections to the electronic energies for 298 K were scaled by 0.96. More accurate single point energies were obtained using the 6-311+G(2d,p) basis set for all atoms, except Pd for which the LANL2DZ basis set incremented by four sets of 4f polarization functions was applied.[21]

Mizoroki–Heck and hydrogenation reactions

A typical Heck reaction of iodobenzene and methyl acrylate was carried out in a 50 ml laboratory reactor. The reactor was charged with 0.05 g of supported palladium catalyst, 0.28 ml of iodobenzene, 0.23 ml of methyl acrylate, 0.15 ml of toluene, 0.35 ml of triethylamine and 1.00 ml of *N*-methylpyrrolidone (NMP). The reaction was conducted at 80°C for 1.5 h. The reaction of bromobenzene with styrene was carried out in a 50 ml laboratory reactor. This reaction was carried out under standard conditions (0.1 mol% of supported palladium catalyst, 10 mmol of bromobenzene, 15 mmol of styrene, 12 mmol of sodium acetate (NaOAc) as a base and 10 ml of NMP). The reaction was conducted at 140°C for 6 h. The reaction of iodobenzene and *n*-butyl acrylate was carried out in a 50 ml laboratory reactor. The reactor was charged with 0.1 mol% of supported palladium catalyst. The Heck coupling of 2 mmol of iodobenzene with 2.8 mmol of *n*-butyl acrylate in 3.00 ml of NMP was used as a model system. Triethylamine (2.5 mmol) was additionally used as a base. The reaction was conducted at 130C for 30 min.

The hydrogenation reactions were carried out in a 100 ml Parr reactor (model 4593) with a glass liner. A typical hydrogenation run was as follows. The reactor was charged with 0.2 g of supported palladium catalyst, 5 ml of 96% ethanol, 0.25 ml of toluene and 0.25 ml of cinnamaldehyde or crotonaldehyde. The reactor was flushed several times with pure hydrogen and then the hydrogen pressure and temperature were adjusted to the required level: 40 bar and 75°C for cinnamaldehyde and 90°C for crotonaldehyde. The product was identified by matching retention times with those of pure compounds. In both recycling tests, when reactions were completed, the catalyst was separated, washed with toluene (3 × 25 ml), vacuum dried and used for the next reaction. The product was identified by matching retention times with those of authentic samples.

Mercury test

The mercury poisoning experiment was performed using 500-fold excess of Hg(0) relative to palladium catalyst. Supported catalyst was stirred with mercury for 24 h prior to reaction. The same experiment was also conducted as a reference, using as catalyst the homogeneous complex $PdCl_2(PhCN)_2$. In this case, Hg(0) was introduced at the beginning, together with other reactants.

Results and discussion

Characterization of polymer supports and immobilized Pd catalysts

PTU hardeners were prepared and characterized according to our earlier paper.[17] By the incorporation of thiol groups into the epoxy matrix we obtain a polymer chain with ligands able chelate the palladium complex via ligand exchange reaction. This procedure leads to a controlled introduction of bonding groups to the support structure.

FT-IR spectroscopy was used to confirm the chemical structure of polymer matrices and polymer-supported catalysts. Figure 3 shows FT-IR spectra of epoxy resin cured with MPTU and catalyst EP5/MPTU/Pd. The presence of thiourethane linkages is confirmed by the characteristic peak at 1506 cm^{-1}. The lack of absorption

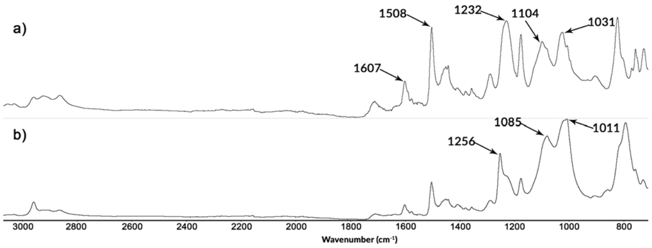

Figure 3. FTIR spectra of (a) EP5/MPTU and (b) EP5/MPTU/Pd.

peaks of S–H vibration at 2545 cm^{-1} and isocyanate group at 2272 cm^{-1} shows the quantitative polyaddition of thiol and isocyanate groups. In our view, the peak at 1085 cm^{-1} in the spectrum of EP5/MPTU/Pd catalyst indicates that oxygen atoms of the epoxy ring can participate in the metal coordination to the polymer matrix. The stretching vibration of the C=O group of the urethane combined with strong absorption of N–H at 1256 cm^{-1} and the presence of characteristic urethane bands at 1607 cm^{-1} give proof for the urethane cross-linking process. The shifts in the intensity ratio of these bands can indicate an interaction between the nitrogen atom and the transition metal. The characteristic vibration of the Pd–S bond cannot be detected in the FT-IR spectrum.

XPS analysis of the outer surface of the particles makes it possible to obtain relevant information about the metal coordination to the polymer matrix and the mechanism of the catalytic reaction. The observed XPS (Table 1) binding energy peak of Cl 2p$_{3/2}$ in the region of 198.22–200.81 eV indicates the presence of $PdCl_2$ structure. The fractions of palladium nanoclusters are also observed, which form due to the overlapping side of the d atomic orbitals. The XPS data summarized in Table 1 show that three possible coordination states (oxygen, nitrogen, sulfur atoms) participate in binding Pd to epoxide support. The XPS spectra of EP5/PTU/Pd catalysts show that palladium appears predominantly in the form of Pd(II). This indicates that these polymeric support chains might stabilize catalytically active monovalent metastable species with a binding energy larger than that of Pd metal. Since the epoxide matrix cured with PTU hardener possesses coordination sites of different coordination ability, it seems likely that the zero-valent palladium, Pd(0), comes from the reduction of Pd(II) coordinated to three possible coordination sites.[22,23]

Table 1. Binding energy values from XPS measurements

Catalyst	Element	Binding energy (eV)	Chemical states
EP5/MPTU/Pd	O 1s	533.61	C=O
		534.89	C–O–C
	N 1s	404.13	N–C(O)
	S 2p	163.28	S–H
		164.70	S–C
	Cl 2p	200.81	$PdCl_2$
	Pd 3d$_{5/2}$	—	Pd(0)
		337.03	Pd(II)
		335.19	Pd$^{\delta+}$
EP5/MPTU/Pd after use	Pd 4f$_{7/2}$	336.02	Pd(0)
		337.01	Pd(II)
		335.04	Pd$^{\delta+}$
EP5/DPTU/Pd	O 1s	533.31	C=O
		534.75	C–O–C
		536.78	–O– epoxy ring
	N 1s	402.68	N–C(O)
	S 2p	163.33	S–H
		164.59	S–C
	Cl 2p	198.22	$PdCl_2$
	Pd 3d$_{5/2}$	—	Pd(0)
		337.62	Pd(II)
		336.34	Pd$^{\delta+}$
EP5/DPTU/Pd after use	Pd 3d$_{5/2}$	336.61	Pd(0)
		337.50	Pd(II)
		335.38	Pd$^{\delta+}$

Quantum chemical calculations

DFT methods were employed to get a deeper insight into the structures of palladium–thiourethane complexes. We performed calculations of the structures and binding energies for the simplified models (Scheme 1).

PTUs contain three atoms, oxygen, nitrogen and sulfur, capable of coordinating to transition metals. We examined the possibility of intramolecular (Scheme 1(B)) and intermolecular (Schemes 1(A) and (C)) binding for both *cis* and *trans* palladium complexes (Scheme 2). The enthalpy of formation of $PdCl_2L_2$ from $PdCl_2$ and model fragments of thiourethane chains strongly depends on the coordinating atom involved, ranging from −83.8 kcal mol^{-1} for S–Pd–S to −72.5 kcal mol^{-1} for O–Pd–O to −72.6 kcal mol^{-1} for N–Pd–N systems. The Pd–Cl and Pd–L bond lengths and Cl–Pd–L angles (where L = S-, N-, O-coordinating ligands) in optimized structures are consistent with the literature for similar systems. Small molecular crystal structures of complexes of $PdCl_2$ with sulfur[24,25] or nitrogen[26,27] ligands are well characterized, but, to our knowledge, there are no such structures involving carbonyl oxygen ligands. Therefore, we compared similar systems (Pd is coordinated to four oxygens in β-diketones or acetic acids).[28,29] The comparison is presented in Table 2.

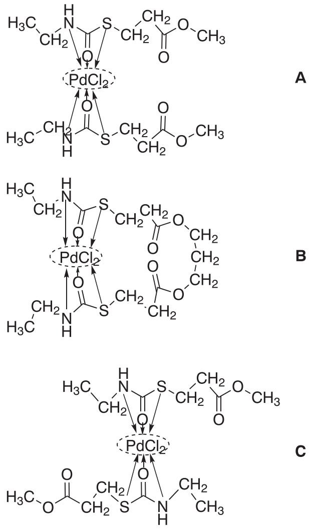

Scheme 1. Structure of binding of palladium with polymer: (A) intermolecular – head-to-head; (B) intramolecular – head-to-head; (C) intermolecular – head-to-tail.

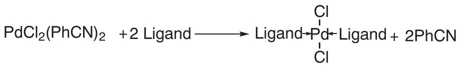

$$PdCl_2(PhCN)_2 + 2\,\text{Ligand} \longrightarrow \text{Ligand}-\overset{Cl}{\underset{Cl}{Pd}}-\text{Ligand} + 2PhCN$$

Scheme 2. Ligand exchange between $PdCl_2(PhCN)_2$ and fragments of PTU chain.

Copyright © 2015 John Wiley & Sons, Ltd.

Table 2. Selected bond distances (Å) and angles (°) for *trans* form of examined structure

	DFT calculation			Literature data		
	Pd–L	Pd–Cl	L–Pd–Cl	Pd–L	Pd–Cl	L–Pd–Cl
O ligands	2.09	2.36	88.97 91.06	2.05 2.02	—	89.9[a] 90.1[a]
N ligands	2.15	2.36	86.69 93.3	2.07	2.3	88.91 91.12
S ligands	2.42	2.37	87.43 92.66	2.32	2.29	84.47 95.53

[a]–O–Pd–O angle.

The distance from cross-linking node in the net also significantly affects the Pd–L bond strength. The closer the node is, the greater is the steric hindrance, and the lower is the binding energy. The influence of the distance from the cross-linking node has been tested for the longer chain structure and palladium coordination to S ligands. Enthalpy of ligand exchange is −15.7 kcal mol^{-1} and is slightly smaller than that of intermolecular binding (−18.6 kcal mol^{-1}). The head-to-head or head-to-tail arrangement of thiourethane chain fragments has little meaning (Schemes 1(A) and (C)). It is worth noting that *cis*-$PdCl_2L_2$ is less stable than the *trans* form by 10 kcal mol^{-1} for oxygen and sulfur and by about 4 kcal mol^{-1} for nitrogen (Table 3; Scheme 2). To model the interactions of Pd with thiourethanes, we have calculated the enthalpy of ligand exchange between $PdCl_2(PhCN)_2$ and fragment PTU chains containing appropriate groups (Table 3; Scheme 2). The dimeric structures of $PdCl_2$ with sulfur are known[24] but there is no information on the corresponding systems with nitrogen and oxygen atoms (Scheme 3). Calculations show that such connections are possible, but the formation of the 'dimeric' complex in a reaction analogous to that shown in Scheme 2 is less favourable than the formation of the 'monomeric' complex (Scheme 1). However, in excess of $PdCl_2$, the formation of the dimer seems probable. The difference in enthalpy of formation of one Pd–Cl and one Pd–L bond and enthalpy of formation the two Pd–L bonds is 7–15 kcal mol^{-1}.

Table 3. Enthalpy of ligand exchange for the tested structures

	ΔH (kcal mol^{-1})		
Structure	O–Pd–O	N–Pd–N	S–Pd–S
trans-form Head-to-head (Scheme 1(A))	−7.28	−7.43	−18.63
trans-form Head-to-tail (Scheme 1(C))	−7.65	−7.05	−19.95
trans-form Intramolecular (Scheme 1(B))	17.92	18.58	−4.49 (−15.7[a])
cis-form Head-to-head (Scheme 2)	3.31	−4.01	−8.83
Dimeric structure (Scheme 3)	1.15	0.46	−6.76

[a]Longer chain structure (see supporting information).

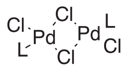

Scheme 3. Structure of palladium chloride dimer.

Catalytic study

Mizoroki–Heck reaction

The activity and stability of the supported catalysts were tested in Mizoroki–Heck (Scheme 4) and hydrogenation (Scheme 5) reactions. The Heck reaction is one of the most important methods for carbon–carbon bond formation in organic chemistry. It is used in a wide variety of organic transformations and thus it now belongs to an indispensable set of palladium-catalysed cross-coupling reactions. Therefore activity and stability of the supported catalysts were tested in Mizoroki–Heck coupling of iodobenzene and methyl acrylate (Scheme 4). The only observed product is methyl *trans*-cinnamate. Kinetics of reaction was followed with GC, by withdrawing samples at certain time intervals (Fig. 4). The prepared catalysts were also tested for other substrates. All catalysts used show high activity and selectivity in the Heck coupling of bromobenzene with styrene (conversions: 73–82%; selectivities: 83–85%). Moreover, activities in the transformation of activated bromobenzene are also satisfactory. In the reactions complete *E* selectivity is observed, whereas in the transformations of styrene, products of a coupling are found. It is also seen that activities depend on palladium loadings and parallel metal dispersion. For very low palladium concentrations of 0.1 mol%, *trans*-stilbene is observed as the main product in all cases. The selectivity is very similar for both catalysts (*trans*-stilbene:*cis*-stilbene:1,1-diphenylethene = 90:2:7) and comparable to that for typical homogeneous systems.

The scope of iodobenzene and *n*-butyl acrylate to give *n*-butyl cinnamate was also examined for the Heck cross-coupling reaction. In this case we obtain a high efficiency. The reaction proceeds smoothly to completion within 30 min at 130°C to afford the desired product in 79% isolated yield. Employing the optimized catalytic

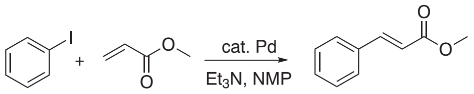

Scheme 4. Model Heck reaction.

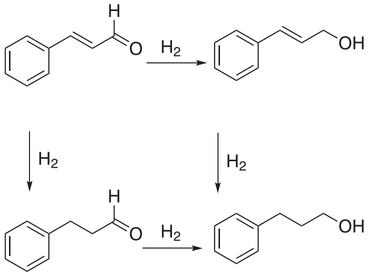

Scheme 5. Hydrogenation of cinnamaldehyde.

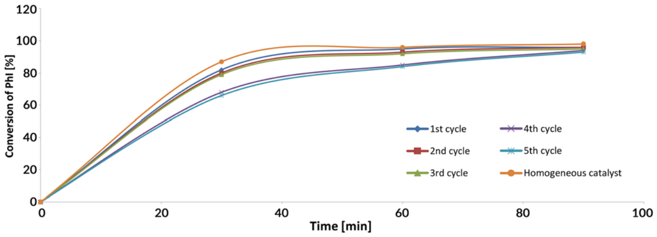

Figure 4. Kinetics of reaction of iodobenzene with methyl acrylate catalysed by EP5/MPTU/Pd and kinetics of reaction catalysed by $PdCl_2(PhCN)_2$.

conditions, iodobenzene with *n*-butyl acrylate provide excellent yields of the desired products in very short reaction times. Products of both reactions were followed using GC. The results confirm that prepared catalyst could be used in many organic reactions. In this work we present detailed results only for reaction of iodobenzene and methyl acrylate because this reaction gives good results, does not need to be conducted at temperatures above 80°C and we observe only one product of the reaction.

Hydrogenation reaction

The second reaction investigated, the selective hydrogenation of α,β-unsaturated carbonyl compounds to their corresponding unsaturated alcohols, is an important step in the preparation of various fine chemicals such as fragrances for the perfume and pharmaceutical industries. Hydrogenation reaction of cinnamaldehyde can give three products, namely hydrocinnamaldehyde (HCALD), cinnamyl alcohol (CALC) and hydrocinnamyl alcohol (HCALC). The mostly desired product is the α,β-unsaturated alcohol (CALC) which is difficult to produce in a catalytic hydrogenation of α,β-unsaturated aldehydes because the hydrogenation of C=C bonds in the presence of noble metals is thermodynamically and kinetically favoured over the hydrogenation of the C=O bonds. The results (Table 4) show that the morphology, chemical structure of the polymeric matrix and way of immobilization influence the selectivity of this reaction. The selectivity of this reaction strongly depends on the types of binding groups present in the polymer. Results presented in Table 4 show that for both tested catalysts there is a significant difference in the product distribution between the first and fifth runs. This is probably caused by easier access of substrates to the active sites in the open pores of the catalyst.

The activity and selectivity of the prepared catalysts were also examined for liquid-phase hydrogenation of crotonaldehyde (CAL). The reaction gives a mixture of saturated aldehyde (butyraldehyde – SAL), saturated alcohol (butanol – SOL) and crotyl alcohol (UOL). Also the diacetal 1,1-diethoxybutane (DA) is produced in the side reaction between CAL and ethanol used as a solvent. Results presented in Table 5 show that in both cases the catalyst selectivity towards UOL is increased after each catalytic cycle. The higher selectivity to UOL is the result of a large increase in the rate of the hydrogenation of the C=O group. A higher selectivity to UOL means a low selectivity for the hydrogenation of the C=C bond. What is more, a fast conversion of CAL to UOL also means a low yield of DA.

Table 4. Hydrogenation of cinnamaldehyde over EP5/MPTU/Pd and EP5/DPTU/Pd[a]

			Distribution of reaction products		
Catalyst	Run	Conversion (%)	HCALD (%)	HCALC (%)	CALC (%)
Homogeneous $PdCl_2(PhCN)_2$	1	98	13	76	11
EP5/MPTU/Pd	1	98	9	66	25
	2	98	8	65	27
	3	97	7	73	20
	4	97	3	79	18
	5	97	3	80	17
EP5/DPTU/Pd	1	96	7	60	33
	2	96	6	63	31
	3	96	5	78	17
	4	95	2	83	15
	5	95	3	95	2

[a]Conditions: temperature, 75°C; time, 4 h; solvent, 96% ethanol; overall volume, 5.5 ml. Unidentified reaction products are not shown.

Table 5. Hydrogenation of crotonaldehyde over EP5/MPTU/Pd and EP5/DPTU/Pd[a]

			Distribution of reaction products				
Catalyst	Run	Conversion (%)	CAL (%)	SAL (%)	SOL (%)	UOL (%)	DA (%)
Homogeneous $PdCl_2(PhCN)_2$	1	98	14	86	—	—	—
EP5/MPTU/Pd	1	98	25	11	12	28	24
	2	98	25	11	15	29	20
	3	98	18	11	21	31	19
	4	97	10	10	27	34	19
	5	97	7	10	30	35	18
EP5/DPTU/Pd	1	96	25	9	11	27	28
	2	96	23	9	16	25	27
	3	96	16	10	24	29	21
	4	95	10	12	29	37	12
	5	95	5	13	31	39	12

[a]Conditions: temperature, 90°C; time, 8 h; solvent, 96% ethanol; overall volume, 5.5 ml. Unidentified reaction products are not shown.

The nitrogen BET adsorption method results (Table 6) indicate that the investigated supports have different pore size distributions which probably arise from differences in their cross-link densities. The EP5/MPTU resin exhibits a lower value of average pore size, lower surface area and lower porosity than EP/DPTU support. For all supports, immobilization of palladium precursor results in a similar loss in surface area and corresponding decrease in mean pore size diameter. The characterization of palladium distributions on the surface of the catalysts was performed using SEM and EDX for samples of catalysts after fifth use (Fig. 5). The noticeable different microporous structures of the DPTU- and MPTU-cured resins presented in Fig. 5 can influence the activity of catalyst by the steric demands of a catalytic centre bound to these supports. From the presented SEM-EDX images of the catalysts it is difficult to precisely

Table 6. Characteristics of polymer supports and supported Pd catalysts obtained using BET methods

	EP5/ MPTU	EP5/ MPTU/Pd	EP5/ DPTU	EP5/ DPTU/Pd
Surface area ($m^2 g^{-1}$)	88	82	59	51
Average pore diameter (nm)	24	19	9	3
Volume of pores (%)				
Macro $w > 50$ nm	16.9	15.3	13.8	11.2
Meso $2 < w < 50$ nm	67.3	66.1	19.3	17.1
Micro $w < 2$ nm	15.8	18.6	66.9	71.7
Pore specific volume ($cm^3 g^{-1}$)	0.22	0.33	0.31	
Porosity	0.25	0.36	0.12	0.15

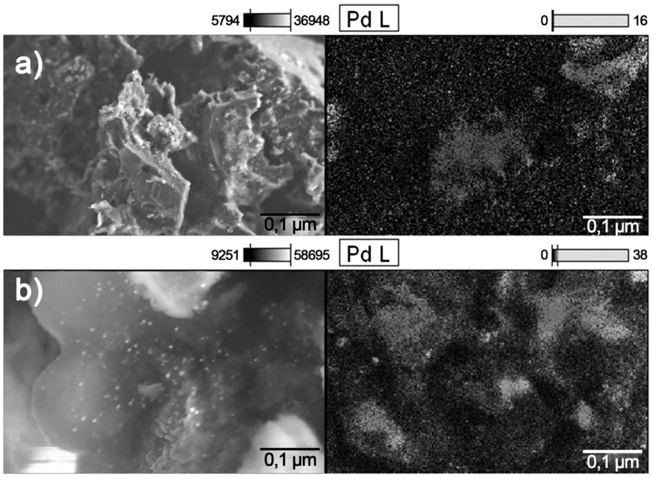

Figure 5. SEM micrographs and EDX Pd-mapping of surface of thiol resin-supported palladium catalysts after fifth use.

characterize Pd clusters or nanoparticles. However, X-ray microprobe analysis shows that Pd is homogeneously dispersed throughout the particles of the EP5/MPTU/Pd and EP5/DPTU/Pd catalysts, suggesting the pore structure in these samples is not favourable for stabilization of Pd (Fig. 6). There are agglomerates of Pd (2–20 nm) dispersed on the surface of resin which indicate that different metal particle size distribution is influenced by the morphology of the support used. This can be also an explanation for the unequal catalyst performances.

The possibility of recycling five times the immobilized palladium catalysts demonstrates their high stability despite the changes that occur in their structure during the catalytic reaction. Selective mercury poisoning was used to exclude the possibility of the reaction being catalysed by unbound palladium metal which is the result of elution of the complex from the surface of the carrier. This method is commonly used to define the nature of a homogeneous or heterogeneous reaction.[30–33] The EP5/MPTU/Pd and EP5/DPTU/Pd catalysts were exposed to mercury and then subjected to the catalytic tests. The examined catalytic activity is similar to that against mercury poisoning. The mercury test was also done for the homogeneous complex $PdCl_2(PhCN)_2$. In this case, addition of Hg(0) to the homogeneous reaction mixture causes the reaction to stop. The results indicate that catalysis is not associated with leached precursor complexes or *in situ* formed palladium nanoclusters, which would be deposited to the polymer matrix after the reaction. The mercury poisoning test shows that metal complex eluted or *in situ* formed palladium nanoclusters do not affect the catalytic activity. Mercury poisoning occurs by a permanent adsorption on and reaction of mercury with catalyst which results in a catalytically inactive compound.

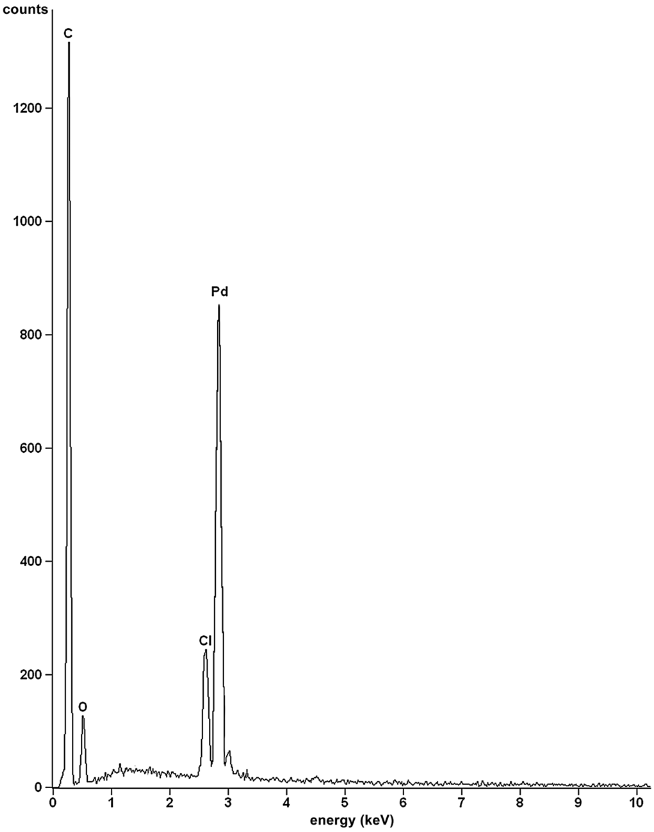

Figure 6. SEM-EDX composition of Pd.

Table 7. Catalyst activity in Heck reaction

Catalyst	Run	$^{106}Pd^+$ intensity of emission[a]	Conversion (%)[b]	Pd content ($mmol\,g^{-1}$)[c]
Homogeneous $PdCl_2(PhCN)_2$	1	—	98	—
EP5/MPTU/Pd	1	7.4×10^{-3}	96	0.0019
	2	—	96	—
	3	—	95	—
	4	—	94	—
	5	5.2×10^{-3}	93	0.0013
EP5/DPTU/Pd	1	4.7×10^{-3}	85	0.0017
	2	—	84	—
	3	—	82	—
	4	—	80	—
	5	3.5×10^{-3}	79	0.0011

[a] Normalized intensity of $^{106}Pd^+$ selected from the mass spectra of palladium catalysts (ToF-SIMS).

[b] Conversion of iodobenzene after 1.5 h. Temperature: 80°C. Substrates: iodobenzene, 0.28 ml (2.5 mmol); methyl acrylate, 0.23 ml (2.5 mmol). Solvent: toluene, 0.15 ml (1.4 mmol); triethylamine, 0.35 ml (2.5 mmol); NMP, 1.00 ml (10.4 mmol). Supported catalyst: 0.05 g. The only observed product was methyl *trans*-cinnamate.

[c] Amount of palladium loaded in the support determined using AAS.

ToF-SIMS and AAS were applied to examine the deactivation process (Table 7). The ToF-SIMS method enables the evaluation of the chemical composition of the catalyst surface. This measurement is useful to define the nature of interactions between metallic phases and supports as well as the distribution of metal or other catalyst components on the surface. In this case, catalysts after the fifth use were investigated and compared to the fresh, unused samples. Only a very small decrease of the amount of surface-available palladium is observed; however, the decrease of palladium content is at such a level that it does not significantly affect the catalyst activity.

Conclusions

The new thiol-functionalized epoxy resin is a very useful polymeric support for the preparation of heterogenized palladium catalysts.

The possibilities of intra- and intermolecular binding for both *cis* and *trans* palladium isomers were examined. The properties of the heterogenized catalysts are due to the chemical structure of the matrix and coordination surrounding the metal centres. Epoxy–metal complex is formed by the interaction of a polymer containing coordinating groups with metal ions. The variety of coordination sites in the prepared polymer support promotes the formation of active catalytic species mainly as finely dispersed metal particles with mixed valence states. Catalytic activity of the prepared supports immobilized with palladium complex was tested in the Heck and hydrogenation reactions. The activity of the catalyst was comparable to that of homogeneous $PdCl_2(PhCN)_2$ complex and remained constant through five reaction cycles. ToF-SIMS, AAS and SEM-EDX measurements gave additional information about surface properties of the supported catalysts. The SEM-EDX results showed that for all tested catalysts, palladium was equally distributed on the surface of the thiol–epoxy supports. The differences in activity were caused by dissimilarity in the chemical structure of the prepared supports, as well as the other effects of surface morphology of supports cross-linked with different type of new hardeners. The results of the research gave more information about the possible interaction of Pd(II) complexes with epoxy resin cured with PTUs containing oxygen, nitrogen and sulfur atoms which can bind transition metals. The chemical structure of the matrix and coordination surrounding the metal centres have a significant effect on catalytic properties of the heterogenized catalysts. Such thiol-functionalized epoxy resin is being explored for many different applications, especially in catalysis, where palladium can effectively catalysts a range of different transformations.

Acknowledgments

This research was supported in part by PL-Grid Infrastructure.

References

[1] H. Q. Pham, M. J. Marks, Epoxy resins. in *Ulmann's Encyclopedia of Industrial Chemistry*, Wiley-VCH, Weinheim, **2006**.
[2] S. Han, H. G. Yoon, K. S. Suh, W. G. Kim, T. J. Moon, *J. Polym. Sci.* **1999**, *37*, 713.
[3] S. J. Park, M. K. Seo, J. R. Lee, D. R. Lee, *J. Korean Fiber Soc.* **1999**, *36*, 715.
[4] S. T. Oyama, *Mechanisms in Homogeneous and Heterogeneous Epoxidation Catalysis*, Elsevier Science, New York, **2008**.
[5] V. Grazu, O. Abian, C. Mateo, F. Batista-Viera, R. Fernandez-Lafuente, J. M. Guisan, *Biotechnol. Bioeng.* **2005**, *90*, 597.
[6] C. Zhang, X. Li, J. Pang, *J. Appl. Polym. Sci.* **2001**, *82*, 1587.
[7] S. Y. Lee, M. Yamada, M. Miyake, *Sci. Technol. Adv. Mater.* **2005**, *6*, 420.
[8] F. Lu, J. Ruiz, D. Astruc, *Tetrahedron Lett.* **2004**, *45*, 9443.
[9] J. Alvarez, J. Liu, E. Román, A. E. Kaifer, *Chem. Commun.* **2000**, 1151.
[10] R. Tatumi, T. Akita, H. Fujihara, *Chem. Commun.* **2006**, 3349.
[11] K. Strzelec, N. Bączek, M. Szynkowska, J. Grams, *J. Appl. Polym. Sci.* **2014**, *131*, 40330.
[12] C. J. Cramer, D. G. Truhlar, *Phys. Chem. Chem. Phys.* **2009**, *11*, 10757.
[13] M. Atanasov, C. A. Daul, *Chimia* **2005**, *59*, 504.
[14] Y. Minenkov, Å. Singstad, G. Occhipinti, V. R. Jensen, *Dalton Trans.* **2012**, *41*, 5526.
[15] A. T. Bell, M. Head-Gordon, *Annu. Rev. Chem. Biomol. Eng.* **2011**, *2*, 453.
[16] F. R. Hartley, *The Chemistry of Platinum and Palladium*, Applied Science Publishers, London, **1973**.
[17] K. Strzelec, N. Bączek, S. Ostrowska, K. Wąsikowska, M. I. Szynkowska, J. Grams, *C. R. Chimie* **2012**, *15*, 1065.
[18] M. J. Frisch, G. W. Trucks, H. B. Schlegel, G. E. Scuseria, M. A. Robb, J. R. Cheeseman, J. A. Montgomery, Jr., T. Vreven, K. N. Kudin, J. C. Burant, J. M. Millam, S. S. Iyengar, J. Tomasi, V. Barone, B. Mennucci, M. Cossi, G. Scalmani, N. Rega, G. A. Petersson, H. Nakatsuji, M. Hada, M. Ehara, K. Toyota, R. Fukuda, J. Hasegawa, M. Ishida, T. Nakajima, Y. Honda, O. Kitao, H. Nakai, M. Klene, X. Li, J. E. Knox, H. P. Hratchian, J. B. Cross, V. Bakken, C. Adamo, J. Jaramillo, R. Gomperts, R. E. Stratmann, O. Yazyev, A. J. Austin, R. Cammi, C. Pomelli, J. W. Ochterski, P. Y. Ayala, K. Morokuma, G. A. Voth, P. Salvador, J. J. Dannenberg, V. G. Zakrzewski, S. Dapprich, A. D. Daniels, M. C. Strain, O. Farkas, D. K. Malick, A. D. Rabuck, K. Raghavachari, J. B. Foresman, J. V. Ortiz, Q. Cui, A. G. Baboul, S. Clifford, J. Cioslowski, B. B. Stefanov, G. Liu, A. Liashenko, P. Piskorz, I. Komaromi, R. L. Martin, D. J. Fox, T. Keith, M. A. Al-Laham, C. Y. Peng, A. Nanayakkara, M. Challacombe, P. M. W. Gill, B. Johnson, W. Chen, M. W. Wong, C. Gonzalez, J. A. Pople, *Gaussian 03, Revision D.01*, Gaussian Inc, Wallingford, CT, **2004**.
[19] D. Young, *Computational Chemistry*, Wiley-Interscience, New York, **2001**, Appendix A.1.6, Spartan, p. 330.
[20] Y. Zhao, D. G. Truhlar, *Theor. Chem. Acc.* **2008**, *120*, 215.
[21] G. T. de Jong, M. Sola, L. Visscher, F. M. Bickelhaupt, *J. Chem. Phys.* **2004**, *121*, 9982.
[22] A. Biffis, M. Zecca, M. Basato, *J. Mol. Catal. A* **2001**, *173*, 249.
[23] A. F. Schmidt, A. Halaiqa, L. O. Nindakova, O. S. Skripina, *React. Kinet. Catal. Lett.* **1999**, *67*, 301.
[24] M. Basato, A. Cardinale, M. Zecca, G. Valle, *Inorg. Chim. Acta* **2000**, *303*, 100.
[25] Y.-B. Xie, J.-R. Li, Y. Zheng, X.-H. Bu, R.-H. Zhang, *J. Mol. Struct.* **2003**, *645*, 227.
[26] Z. D. Petrovic, M. I. Djuran, F. W. Heinemann, S. Rajkovic, S. R. Trifunovic, *Bioorg. Chem.* **2006**, *34*, 225.
[27] G. Bombieri, G. Bruno, G. Cum, R. Gallo, A. Spadaro, *Inorg. Chim. Acta* **1984**, *86*, 121.
[28] S. D. Kirik, R. F. Mulagaleev, A. I. Blokhin, *Acta Crystallogr. C* **2004**, *60*, 449.
[29] A. N. Knyazeva, E. A. Shugam, L. M. Shkol'nikova, *J. Struct. Chem.* **1970**, *11*, 875.
[30] P. Foley, R. DiCosimo, G. M. Whitesides, *J. Am. Chem. Soc.* **1980**, *102*, 6713.
[31] D. E. Bergbreiter, P. L. Osburn, J. D. Frels, *Adv. Synth. Catal.* **2005**, *347*, 172.
[32] J. A. Widegren, R. G. Finke, *J. Mol. Catal. A* **2003**, *198*, 317.
[33] J. M. Richardson, C. W. Jones, *J. Catal.* **2007**, *251*, 80.

Supporting information

Additional supporting information may be found in the online version of this article at the publisher's web-site.

Copyright © 2015 John Wiley & Sons, Ltd.